Langmuir
Article
pubs.acs.org/Langmuir

Capillary and Surface Effects in the Formation of Nanosharp Tungsten Tips by Electropolishing

M. Kulakov, I. Luzinov, and K. G. Kornev*

School of Materials Science and Engineering, Clemson University, 161 Sirrine Hall, Clemson, South Carolina 29634

Received August 1, 2008. Revised Manuscript Received November 26, 2008

The DC electropolishing process has been applied to the sharpening of tungsten wires in 2 M KOH aqueous solution. Necking of tungsten anodes takes place in the vicinity of the electrolyte−air interface. This results in the creation of two separate wire parts with nanosharp tips. Using image analysis, we demonstrate that the products of electrochemical reactions on the wire surface form a film with distinguishable properties. Experimental estimates of the film density and interfacial tension show that the film is approximately 32 kg/m^3 denser than the surrounding electrolyte and that its interfacial tension is approximately $\sigma \approx 0.2$ mN/m. Using these estimates, we show that the film flow is predominantly driven by capillary forces. We hypothesize that the wire necking is caused by a bidirectional film flow originated from Plateau−Rayleigh instability and inherent to cylindrical films and jets.

1. Introduction

Tungsten wires with nanotips are widely used as samples for atomic probe microscopes,[1] as charge sources in scanning tunneling microscopes,[2−4] and as nanoindentation tips.[5] Among the numerous methods used to sharpen tungsten wires, electropolishing is considered as the most inexpensive, reliable, and easiest to implement technique for obtaining sharp tips with a nanoscale radii of curvature.[6]

DC electropolishing of tungsten wires typically employs an alkali electrolyte. To produce sharp tips, the tungsten wire is connected to a power supply and serves as an anode in the electrochemical cell. By turning the voltage on, one initiates an electrochemical reaction on the wire surface. As suggested in ref 2, corresponding electrochemical reactions on the anode and cathode proceed according to the following equations:

$$6H_2O + 6e^- \rightarrow 3H_2(g) + 6OH^- \quad (1)$$

$$W(s) + 8OH^- \rightarrow WO_4^{2-} + 4H_2O + 6e^- \quad (2)$$

The initial stage of the process corresponds to dissolution of a thin oxide film covering the metal surface. Emission of oxygen accompanies this process of film dissolution.[6] The electropolishing process results in neck formation, which usually takes place in the vicinity of the electrolyte−air interface.[2] Despite the fact that the process has been known for over 50 years,[7] some of its fundamental aspects remain poorly understood, in particular the mechanism of wire necking.[6]

As suggested in the literature, wire necking can be explained in terms of surface and bulk effects. We mention only basic concepts specifying these effects; an interested reader is referred to detailed reviews in refs 2−6. For example, surface effects play a significant role in the chemical etching of glass fibers.[8] In this process, the glass fiber is submerged vertically into etching solution and the created meniscus controls the tip shape by sliding down a pre-etched cone.[8] Alternatively, bulk effects can be attributed to a flow of the anodic reaction products along an immersed wire.[2,7,9] According to this bulk mechanism, wire necking is associated with a transition zone wherein diffusion-limited kinetics of wire dissolution give way to convection-limited kinetics. The fluid constituting the reaction products, in particular WO_4^{2-} ions[10] which are heavier than the electrolyte, flows down along the wire and develops a boundary layer. This flow is classified as a natural convection,[11] and hence, convection-limited kinetics becomes the rate-limiting factor during electropolishing. The radial diffusion of hydroxyls toward the wire surface is hindered in this boundary layer. Immediately underneath the meniscus where the convection is weak, radial diffusion is also impeded. This is because the concentration gradient is small as follows from the boundary condition that the diffusion flux at the meniscus surface is zero. Therefore, in a region somewhere in between in which the boundary layer is not yet well developed, the radial diffusion flux is expected to reach a maximum. Consequently, this maximum is associated with neck formation.

This vortex shedding mechanism has been employed in the modeling of limiting current during electrochemical

*To whom correspondence should be addressed. E-mail: kkornev@clemson.edu.

(1) Miller, M. K.; Smith, G. D. W. *Atom probe microanalysis: principles and applications to materials problems*; Materials Research Society: Pittsburgh, PA, **1989**.
(2) Ibe, J. P.; Bey, P. P.; Brandow, S. L.; Brizzolara, R. A.; Burnham, N. A.; Dilella, D. P.; Lee, K. P.; Marrian, C. R. K.; Colton, R. J. *J. Vac. Sci. Technol., A* **1990**, *8*, 3570.
(3) Zhang, R.; Ivey, D. G. *J. Vac. Sci. Technol., B* **1996**, *14*, 1.
(4) Klein, M.; Schwitzgebel, G. *Rev. Sci. Instrum.* **1997**, *68*, 3099.
(5) Grunlan, J. C.; Xia, X. Y.; Rowenhorst, D.; Gerberich, W. W. *Rev. Sci. Instrum.* **2001**, *72*, 2804.
(6) Xu, D. W.; Liechti, K. M.; Ravi-Chandar, K. *Rev. Sci. Instrum.* **2007**, *78*, 073707.
(7) Müller, E. W.; Tsong, T. T. *Field ion microscopy; principles and applications*; American Elsevier Pub. Co.: New York, **1969**.
(8) Takahashi, K. M. *J. Colloid Interface Sci.* **1990**, *134*, 181.
(9) Melmed, A. J. *J. Vac. Sci. Technol., B* **1991**, *9*, 601.
(10) Kelsey, G. S. *J. Electrochem. Soc.* **1977**, *124*, 814.
(11) Newman, J. *Electrochemical systems*; Prentice-Hall: Englewood Cliffs, NJ, **1972**.

dissolution of plane vertical electrodes and, particularly, tungsten electrodes in KOH solution.[12] However, the approach cannot be directly projected to an axisymmetric case, because it is not clear if the reaction products will flow according to the scenario of natural convection. As an alternative to vortex shedding, the authors of refs 2, 6, and 9 suggested that diffusion of OH ions might play a significant role in the initiation of neck formation.

This study is intended to assess the role of physicsochemical processes which occur in the proximity of the surface of tungsten wires during electropolishing. In particular, early studies suggested that a thin film composed of the products of electrochemical reaction should have distinguishable properties.[2,7,9,13] These studies proposed that the mobility of ions in the film is significantly reduced thus limiting the rate of electrochemical reaction. A lack of experimental data which would support/deny this hypothesis motivated us to look more closely at the dynamics of film formation by examining the flow of reaction products along the wire. Experiments on tungsten wires of different sizes show that the reaction products form a film with properties distinguishable from the surrounding electrolyte. We model this film as a new phase with a small interfacial tension and a density distinguishable from the density of surrounding electrolyte. The density difference and the interfacial tension were estimated using image analysis. Transport mechanisms of the reaction products were identified by analyzing the observed flow fields. Finally, the necking phenomenon was considered as a manifestation of the Plateau−Rayleigh instability of the film.[14,15]

2. Experimental Procedures

The materials used in this study were commercial 99.95% pure tungsten wires (type 1A ASTM F288-96) supplied by Small Parts Inc., Miramar, FL with diameters of 0.5, 0.7, and 1.0 mm. The wires were cut to necessary lengths using a plain metal cutter. During electropolishing, the tungsten wire was connected as an anode to a DC Instek PSS-2005 programmable power supply purchased from Tequipment, Long Branch, NJ. The response time of the power supply is equal to 10 ms. For a cathode, we used austenitic nonhardenable chromium−nickel stainless steel 314 with a relatively large surface area. All experiments were conducted in a 2 M aqueous solution of potassium hydroxide (KOH). The container for the electrolyte was a standard 150 mL laboratory glass beaker. The experimental assembly was mounted on a laboratory bench with no special antivibration features. The vertical position of the wire was precisely controlled by using a calibrated microscope stage. The wire diameter, depth of immersion into the electrolyte (3−10 mm), and applied electric field (3−14 V) were also controlled. Electropolishing was performed at a constant voltage. The electric current in the circuit was monitored and recorded by a specially designed Labview application. The current continuously decreased in a course of electropolishing. Figure 1 shows a typical example of the current versus time dependence. It was noted that the moment when the current reached zero corresponded to breakage of a neck formed between upper and lower parts of the tungsten wire. Therefore, at this moment, the applied voltage was automatically shut down to prevent blunting of the upper wire.

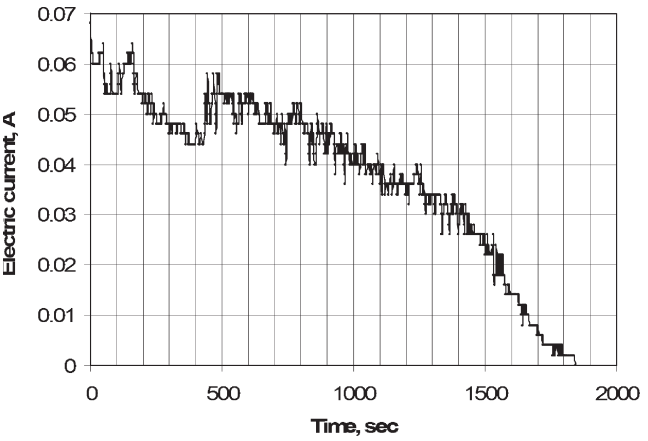

Figure 1. Evolution of electric current during electropolishing of Ø0.7 mm tungsten wire. The length of the immersed part is 5 mm, and the applied voltage is 4 V.

3. Meniscus Behavior

During electropolishing, the tungsten wire was immersed into 2 M KOH solution. The rising liquid column with an upward pointing meniscus indicated wettability of the tungsten surface by the given solution. It appears that the wire part sitting under the meniscus above the flat air−liquid interface was dissolved more quickly compared to the lower part sitting below the flat air−liquid interface. We observed two distinctive meniscus behaviors.

In one case, the meniscus remained in its original position during electropolishing. Figure 2 illustrates this case. A sequence of frames shows the process of electropolishing of Ø0.5 mm tungsten wire when the immersed length is 3 mm and applied voltage is 9 V. This regime resulted in the creation of smooth conically shaped tips. We call this behavior the regime of static meniscus. This static meniscus behavior was typically observed when the wire diameter was equal to or less than 0.5 mm.

In the other case, the meniscus moved in a series of steps toward the flat air−electrolyte interface as seen in Figure 3. This sequence of frames shows electropolishing of Ø0.7 mm tungsten wire when the immersed wire length is 5 mm and applied voltage is 4 V. The stepwise meniscus behavior was typically observed when the wire diameter was greater than 0.5 mm and the applied voltage was less than 9 V. As a result, electropolishing took longer time (10 min and more) compared to electropolishing in the regime of static meniscus. For example, the first leap of the meniscus occurred after ∼25 min of electropolishing (Figure 3), while the process with a static meniscus has been completed in ∼7 min (Figure 2).

This behavior has been associated with the emission of hydrogen bubbles at the cathode. The cathode was positioned at the side of the chamber. When the bubble appeared at the cathode, it subsequently moved up and disturbed the meniscus surface to escape from the electrolyte. In addition, the vertical component of surface tension is reduced at an inclined surface of a polished tungsten tip in a course of electropolishing. Because the number of gas bubbles disturbing the air−electrolyte interface is much greater in the case of prolonged electropolishing, the bubble-induced perturbations are appreciably stronger compared to the regime of static meniscus. The meniscus fell under its own weight and occupied a new position dictated by capillary−gravitational equilibrium. The process was repeated several times, leading to a stepwise meniscus motion during electropolishing. This in turn resulted

(12) Davydov, A. D.; Grigin, A. P.; Shaldaev, V. S.; Malofeeva, A. N. *J. Electrochem. Soc.* **2002**, *149*, E6.
(13) Elmore, W. C. *J. Appl. Phys.* **1939**, *10*, 724.
(14) Plateau, J. *Statique experimentale et theroique des liquides soumis aux seules forces moleculaires*; Gauthier-Villars: Paris, **1873**.
(15) Rayleigh, L. *Philos. Mag.* **1892**, *34*, 145.

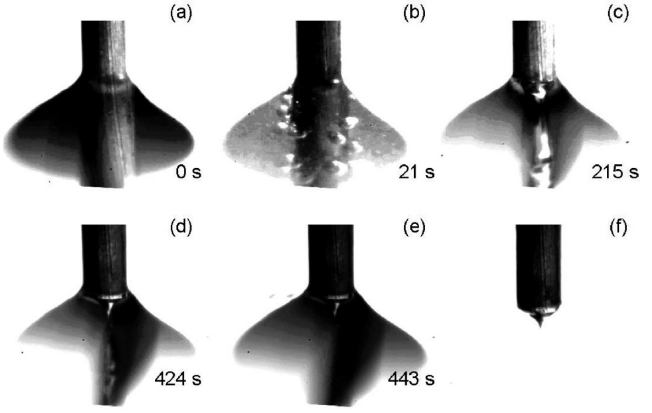

Figure 2. Image sequence showing static meniscus during electropolishing of Ø0.5 mm tungsten wire. The length of the immersed section is 3 mm, and the applied voltage is 9 V.

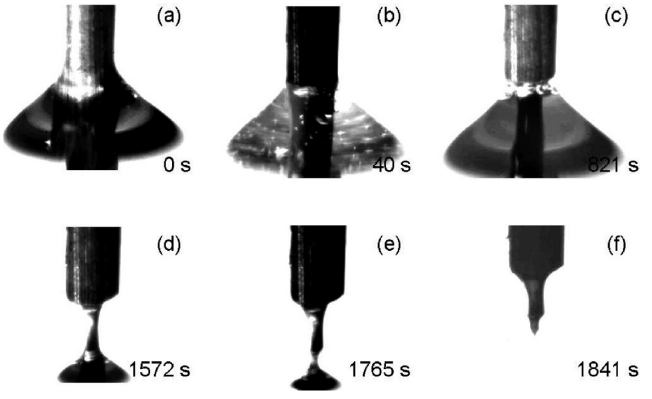

Figure 3. Image sequence showing stepwise meniscus motion during electropolishing of Ø0.7 mm tungsten wire. The length of the immersed part is 5 mm, and the applied voltage is 4 V.

in the formation of a terracelike shape of the tip. Similar meniscus behavior and tip shapes have previously been observed during chemical etching of copper wires.[16]

It is worth mentioning that, at initial stages of electropolishing, bubbling on a wire surface is observed in both regimes of meniscus behavior (Figures 2b and 3b). As discussed in ref 6, these bubbles carry the products of dissolution of tungsten oxides. In both regimes, the electropolishing process leads to neck formation. For example, in the inset of Figure 4, we show a tip with 65 nm radius formed after electropolishing of Ø0.5 mm tungsten wire. The upper part of the wire is short, while the lower part (which detaches and falls down) is more extended, as seen in Figure 4.

The fact that smooth necking has been observed within the meniscus suggests that this phenomenon is caused by physicochemical processes at the proximity of the wire surface. The observed phenomenon does not follow the scenario of the chemical etching which occurs when the meniscus slides over the pre-etched cone.[8,16]

4. Anodic Surface Film

To visualize the flow of reaction products, we used hollow glass particles (Sphericel 60P18, Potters Industries Inc.) with a mean diameter of 18 μm and a density of 600 kg/m^3. Flow was recorded at 100 fps using a Motion ProX3 high-speed camera (Princeton Instruments Inc., Trenton, NJ). An image sequence of the motion of glass particles is shown in Figure 5.

The most intensive movement of the tracers has been observed in the boundary film and in the cylindrical jet as shown in Figure 5. This film is about $t \approx 100\ \mu$m thick. After detachment from the wire end, the jet contracts as the depth increases. The film and jet visibility indicate that they have distinctive physical and chemical properties. Downward motion of the film evolving into the jet suggests that the flowing fluid is denser than the KOH solution. Moreover, the film and the jet with a sufficiently sharp interface imply that the liquids in the film and in the bulk are weakly miscible, at least on the time scales associated with electropolishing. This fact is further supported by surface instabilities observed at the fluid−electrolyte interface (see the Supporting Information). The presence of a thin film with distinct properties has been mentioned in previous studies on electropolishing.[2,7,9,13] This film has also been considered to be highly viscous. The film hypothesis has been put forward to explain the effect of decreased mobility of the products and hydroxyls.[2,7,9,13] We subscribe to this hypothesis. Moreover, we assume that the film has an interfacial tension which supports the film and jet against fast dissolution. The density and the interfacial tension were estimated from the image analysis and electrochemical data. Concentration of WO_4^{2-} ions was assumed to be constant within the film.

4.1. Density Measurements. We take advantage of intensive flow to measure film density. As seen from the images in Figure 5, the film and the jet are well defined and persist for more than 1 s without a significant profile change. This implies that radial diffusion is probably insignificant and that the products of the electrochemical reaction are mostly collected inside the film and the jet. To provide quantitative support for this idea, below we estimate the Peclet number. The Peclet number is a measure of the relative importance of advection with respect to diffusion of WO_4^{2-} ions which constitute the products of electrochemical reaction on the surface of tungsten wire.[2,10] The Peclet number is defined as

$$Pe = \frac{tV}{D} \approx 100 \tag{3}$$

where $t \approx 10^{-4}$ m is the film thickness (Figure 5a), $V = 10^{-3}$ m/s is the average flow velocity of the film, and $D = 10^{-9}$ m^2/s is the diffusion coefficient of WO_4^{2-} ions in KOH solution taken from ref 12.

Since the Peclet number is large, the advection prevails over the diffusion; that is, WO_4^{2-} ions do not have enough time to diffuse away from the film or jet. This is also confirmed by experimental observations of a puddle formed by the flow after stopping the reaction: the puddle does not dissolve for quite a long time (see the Supporting Information). Observations on tracers reveal that the time required for a tracer to pass the field of observation (~1 mm) was only fractions of a second! Therefore, at these time scales, the diffusion is not significant.

Using this idea, the maximum density difference between the film and 2 M KOH solution can be calculated as

$$\Delta\rho_{\max} = \frac{G}{Q} \tag{4}$$

where G is the rate of wire dissolution and Q is the volumetric flow rate.

(16) Bico, J.; Vierling, K.; Vigano, A.; Quere, D. *J. Colloid Interface Sci.* **2004**, *270*, 247.

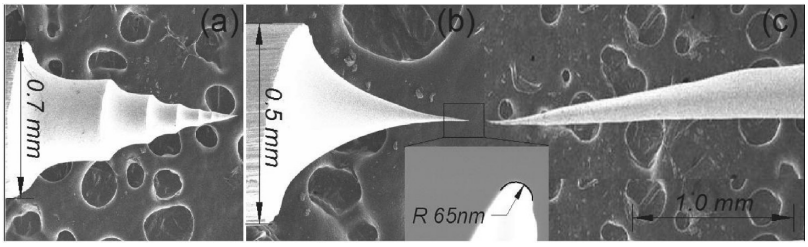

Figure 4. (a) Terracelike and (b) conical shape of the upper part of the wire and (c) lower part of the wire corresponding to (b). Inset: nanotip.

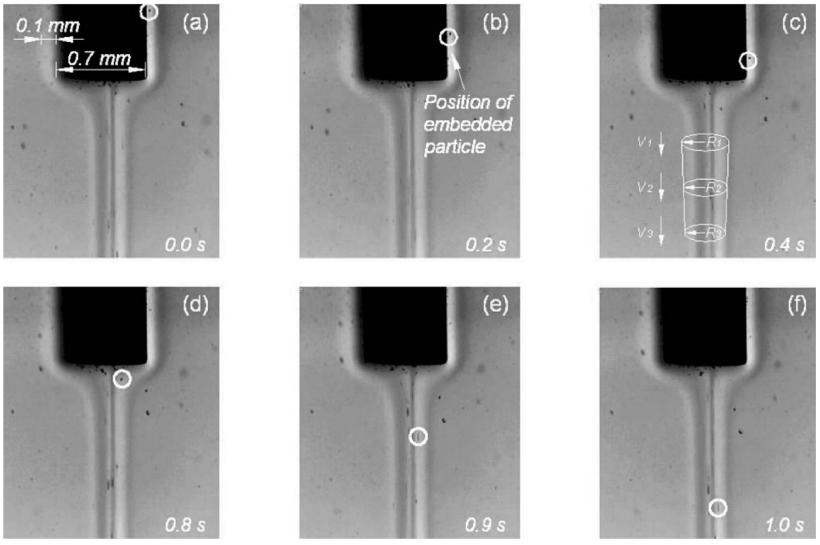

Figure 5. Flow of reaction products as observed by the movement of glass particles along the film and jet. The length of the immersed section of wire is 5 mm, and the voltage is 4 V.

The jet velocity, V_i (after detaching from the wire end), is found by tracing the position of the embedded particles between subsequent frames. We measured the jet radius, R_i, directly from the images as shown in Figure 5c, making approximately $i \approx 10$ measurements at ~0.05 s intervals along the jet height at a constant electric current. Volumetric flow rate was calculated as

$$Q = V_i(\pi \times R_i^2) \tag{5}$$

The flow rate did not vary significantly along the jet height during the experiment, and therefore, it can be assumed constant within the experimental error.

According to Faraday's law,[11] the constant electric current determines the rate of tungsten dissolution during the flow measurements. The current was constant for approximately 20 s (it did not change relative to the minimum increment of the power supply, 0.002 A). Therefore, the rate of wire dissolution when electric current passes through the electrolytic cell is estimated using Faraday's law as

$$G = \frac{IM}{nF} \tag{6}$$

where I is electric current (A), $M = 183$ g/mol (tungsten molar mass), $n = 6$ (tungsten valence number), and F is Faraday's constant, $F = 96485$ mol/C. Using experimental data for electric currents I and flow rates Q (Figure 6), the average density difference calculated from eqs 4−6 is found to be $\Delta\rho = 32$ kg/m^3. Statistical error associated with the average density difference estimations was calculated as the ratio of standard deviation, $\Sigma(\Delta\rho) = 3$ kg/m^3, and the square root of the number of measurements, $n = 12$

$$\Delta(\Delta\rho) = \frac{\Sigma(\Delta\rho)}{\sqrt{n}} \tag{7}$$

The error is equal to 0.9 kg/m^3.

4.2. Surface Tension Measurements. Figure 7a shows that in three sets of measurements conducted at different experimental conditions the jet radius is inversely proportional to the square root of the jet velocity. Therefore, all three experiments show the constant flow rate, $Q = 0.5$ mm^3/s. In addition, Figures 5 and 7b show that there is a linear relation between the jet curvature (which is equal to $1/R$) and vertical coordinate. It appears, therefore, that the jet shape is dictated predominantly by the surface tension and gravity as follows from the pressure balance for a static liquid column:

$$-\Delta\rho g h + \frac{\sigma}{R} = \text{const} \tag{8}$$

where g is gravitational acceleration, h is the distance from the submersed wire end, σ is the interfacial tension at the jet−electrolyte interface, and R is the jet radius.

Equation 8 was compared with the experimental relation between the jet radius, R, and the distance, h, from the submersed wire end (Figure 7b). Experimental data excellently fit the pressure balance (eq 8). The fitting constant in the right-hand side of eq 8 depends on the depth of the wire immersion, while the slope is the same for all three curves. From this slope, we find that the interfacial tension is $\sigma \approx 0.2$ mN/m. Substitution of limiting values of the density

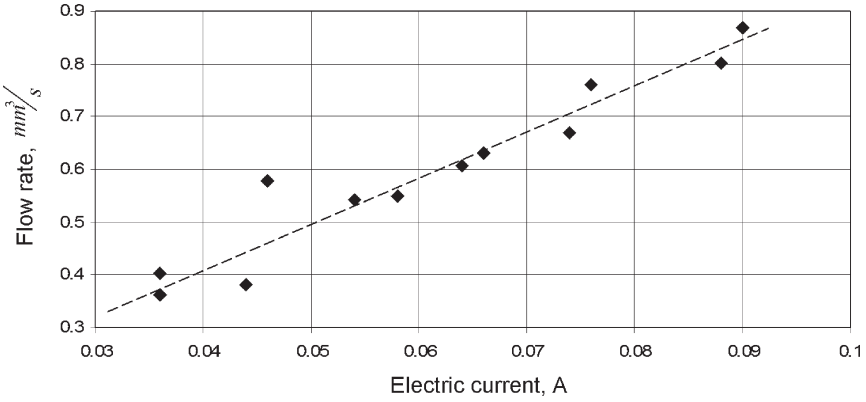

Figure 6. Results of volumetric flow rate and electric current measurements.

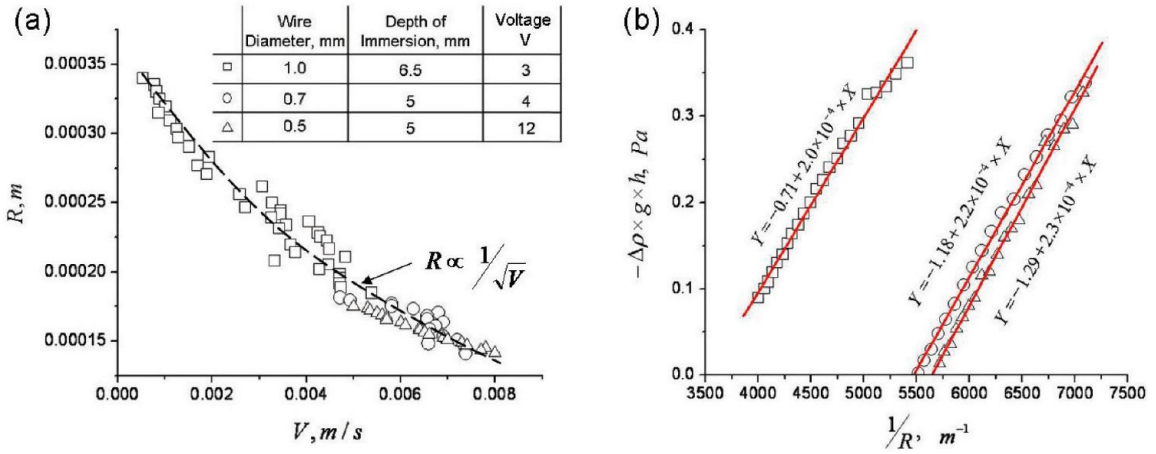

Figure 7. (a) Radius and velocity of the jet after detachment from the wire end; flow rate is $Q = 0.5\,mm^3/s$. Table in (a) describes the experimental conditions. (b) Hydrostatic pressure versus jet curvature for three experiments specified by the table in (a).

difference obtained above according to the statistical error estimation results in experimental error ~0.02 mN/m for the measured surface tension.

4.3. Comparison of Capillary and Gravitational Forces. Let us assume that the wire is covered by the film from the submerged end to the meniscus surface. The effects of gravitational and capillary forces on the film motion can be revealed by estimating the Bond number.[17] When this dimensionless ratio of gravitational to capillary forces

$$Bo = \frac{\Delta\rho g l}{\sigma / r} \tag{9}$$

is greater than 1, the gravitational forces are significant. Otherwise, the gravitational forces are negligible, and the capillary forces play the dominant role in the film flow. Taking as a characteristic length l the maximum distance from the top of the meniscus to the point where the necking takes place, $l \approx 10^{-3}$ m, and as a characteristic radius of the film r the maximum radius of tungsten wire used in the present study, $r = 0.5 \times 10^{-3}$ m, we obtain $Bo = 0.784$. For a smaller initial wire radius, the Bond number will be much smaller than 0.784. This upper estimate of the Bond number shows that, within a region where necking takes place, the capillary forces dominate over the gravitational ones. As the wire radius at the neck approaches zero, the Bond number diminishes, thus indicating a weakening of the gravitational forces in the course of electropolishing. Therefore, the motion of the film constituting the products of electrochemical reaction is mainly caused by capillary forces.

As an illustration, we compare the capillary and hydrostatic pressures developed during electropolishing of Ø0.5 mm tungsten wire. These pressures are measured within 1 mm below the upper point of the meniscus. The neck is formed within this area. Assuming that the film has negligible thickness along the wire length, we calculate the capillary pressure from Laplace law, $\Delta P_c = \sigma(1/R_1 + 1/R_2)$, where R_1 and R_2 are two principal radii of the curvature of the wire after electropolishing. For the present discussions of the flow mechanisms, only the pressure gradient is of consequence. For illustration purposes, absolute value of the reference pressure on the right-hand side of eq 8 can be chosen arbitrary. We choose atmospheric pressure as a reference point for the hydrostatic pressure, that is, $\Delta P_h = -\Delta\rho g(h - h_0)$, where h_0 is a distance between the flat air−liquid interface and the submersed wire end and h is the vertical coordinate at any given point with the origin of coordinates at the submersed wire end. Therefore, the hydrostatic pressure in the film at a level of the flat air−liquid interface is assumed to be zero.

As seen from Figure 8a, even at the beginning of the electropolishing process, when the wire has a cylindrical shape, $R_2 \rightarrow \infty$, the capillary pressure is greater than the

(17) Gennes, P.-G. d.; Brochard-Wyart, F.; Quéré, D. *Capillarity and wetting phenomena: drops, bubbles, pearls, waves*; Springer: New York, **2004**.

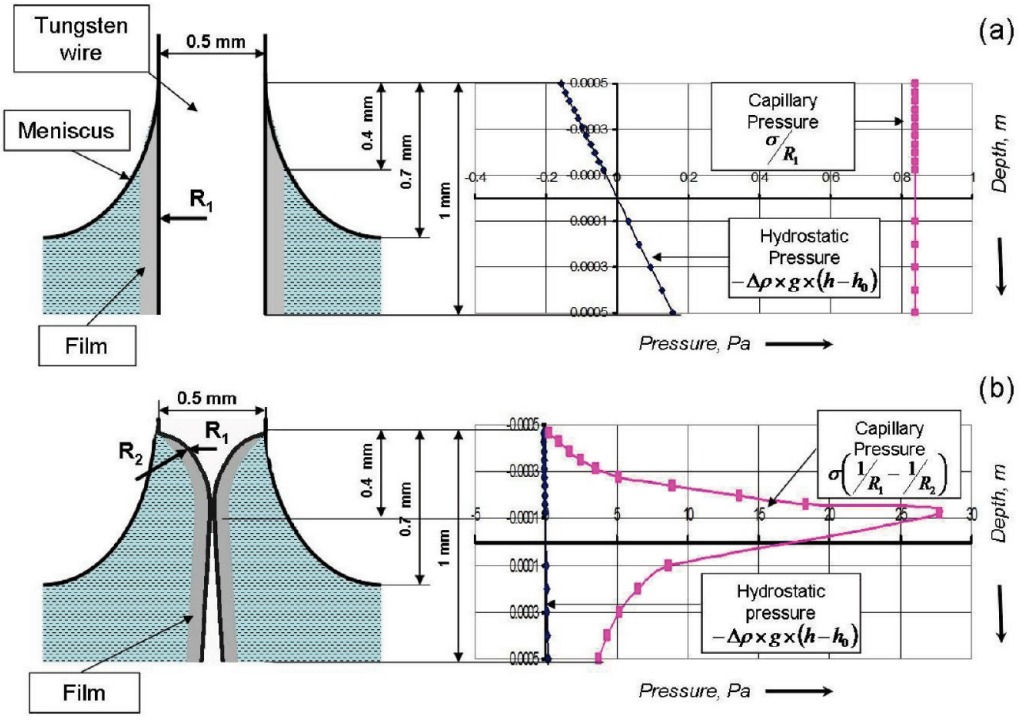

Figure 8. Capillary and hydrostatic pressure distributions during electropolishing of Ø0.5 mm tungsten wire at (a) initial conditions and (b) the final stage of the process. Curvature is calculated using the wire profile in Figure 4b and c.

incremental change in hydrostatic pressure along the submersed section of the wire. As electropolishing progresses, the role of capillary forces becomes increasingly important. In the final stage of the process, despite the fact that the second radius of curvature becomes negative ($R_2 < 0$), the Laplace law predicts that the peak in the capillary pressure distribution at the neck location is many orders of magnitude larger than the hydrostatic component. These considerations confirm the above conclusion that the motion of the fluid film constituting the products of electrochemical reaction is mainly caused by action of the capillary forces.

5. Experimental Modeling of the Necking Phenomenon

On the basis of the experimental results, we propose a new hypothesis which explains the necking phenomenon. This hypothesis originates from past experience with the Plateau−Rayleigh instability inherent in any film covering thin fibers.[14,15] The Plateau−Rayleigh instability states that the cylindrical liquid column of radius r will break up into droplets if the column length l is greater than $l > 2\pi r$. Since capillary forces dominate over other forces acting on the film, similar interfacial instability is expected to develop during electropolishing of tungsten wire. In Figure 9, we show a schematic of the possible flow which leads to neck formation. This schematic is based on the analysis of the pressure distribution shown in Figure 8. The neck presumably coincides with a region where the film splits into upward and downward directed flows. The lower part of the film flows downward, and the variation in rates of the electrochemical reaction is likely caused by gradient of the film thickness not shown in Figure 9. The upper part of the fluid partially follows a circular flow pattern. This stirring process results in intensive mixing of WO_4^{2-} ions and leads to lower rates of electropolishing in the uppermost meniscus region. The flow splitting facilitates removal of the reaction products at the wire neck and increases the rate of neck thinning. It follows, therefore,

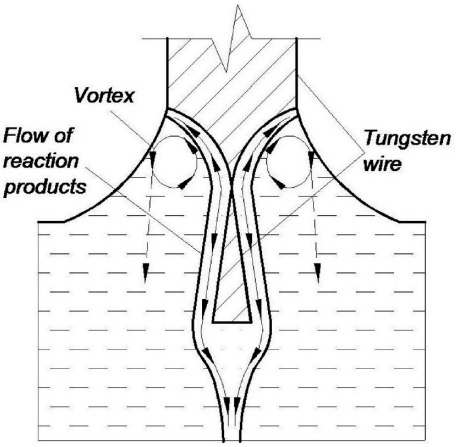

Figure 9. Schematic of the anodic film flow during electropolishing of tungsten wires.

that the necking phenomenon is caused exclusively by flow of the film-constituting products of the electrochemical reaction along the wire surface. The proposed flow pattern is difficult to observe experimentally because of intensive light absorption at the meniscus. Therefore, we conducted a series of experiments modeling the film instability.

Film flow during electropolishing was experimentally modeled using a 3.0 wt % aqueous solution of polyethylene oxide (PEO) (MW = 10^6 Da, Aldrich). Hexadecane was used as a model of light KOH solution. This system has an interfacial tension $\sigma \approx 50$ mN/m. The PEO solution had a density of $\rho_{PEO} \approx 1000$ kg/m^3, and hexadecane ($\rho_{hexadecane}$) = 770 kg/m^3. High viscosity PEO solution was used in anticipation that it will slow down the development of instabilities on the film surface. The PEO−hexadecane system was chosen as a model system to reproduce the immiscibility of fluids and similar

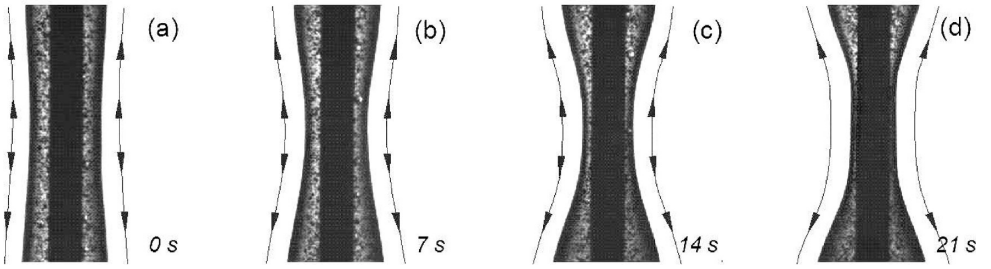

Figure 10. Evolution of 3.0 wt % PEO aqueous film with 0.15 mm initial thickness on Ø0.3 mm tungsten wire immersed in hexadecane for 5 mm.

density difference, yet to enhance the capillary effect. The model is not claimed to be an accurate representation of the combinations of different phenomena taking place during electropolishing. In particular, the effects of wire tapering, gas bubbles, and electrochemical effects are not considered here.

A thin film of PEO was created on Ø0.3 mm tungsten wire by dip coating. The coated wire was then immediately immersed into a reservoir with hexadecane. The film motion was recorded at 30 fps using the high speed camera. A sequence of images of PEO film behavior on tungsten wire is shown in Figure 10. After immersion into hexadecane, the film gradually evolved into droplets separated by regions in which tungsten wire was exposed to hexadecane. The hollow glass particles were uniformly dispersed in the PEO solution for the purpose of observing stream lines. Two separate flows, pointing upward and downward, evolved along the wire surface as indicated by arrows in Figure 10. The region where flow splitting occurs is equally remote from the centers of the future droplets. Bidirectional flow ceased after the droplets found their equilibrium configurations.

Experimental modeling of anodic film behavior during electrochemical polishing of tungsten wires confirms the existence of expected instabilities at the film−electrolyte interface. These instabilities presumably caused splitting of the film flow and eventually resulted in neck formation. Observation of a single neck on a wire is perhaps because of some interplay between the effects of electrochemical reaction and flow. For example, our previous study of thin film instabilities on moving fibers showed that the wavelength of the fastest growing perturbation is influenced significantly by an external flow of a surrounding fluid.[18] Moreover, satellite necks can be dislodged and hence only a single neck can survive. This scenario has been confirmed recently on submillimeter films falling down vertical fibers.[19] Experiments show that the first neck is separated from the wave packet and its development is different from the others. Complete experimental confirmation of the proposed film flow will require sophisticated techniques of flow visualization. The effects of hydrogen bubbles emitted at the cathode should be carefully avoided.

(18) Kornev, K. G.; Neimark, A. V. *J. Colloid Interface Sci.* **1999**, *215*, 381.
(19) Smolka, L. B.; North, J.; Guerra, B. K. *Phys. Rev. E* **2008**, *77*, 036301.

6. Conclusions

Two electropolishing regimes have been observed. In one regime, the meniscus stayed still without visible movements. In another regime, meniscus has been jumping down the wire. It is shown that the static meniscus is associated with the creation of a smooth conical shape of tungsten wire after electropolishing in 2 M KOH electrolyte. Stepwise motion of the meniscus toward a flat air−electrolyte interface was caused by perturbations of the meniscus when gas bubbles protruded through the contact line region during their escape from the electrolyte. This stepwise meniscus motion results in a terrace-shaped tip. Neck formation between the upper and lower parts of the tungsten wire was explained as resulting from the flow of the products of electrochemical reaction on the tungsten wire. These products form a film with distinct properties. The film is about ~32 kg/m^3 heavier than the surrounding electrolyte. The film−electrolyte interfacial tension was estimated to be ~0.2 mN/m. The capillary forces associated with this interfacial tension were found to be primarily responsible for mass transfer of the reaction products. Plateau−Rayleigh instability of the film is suggested as a possible cause of neck formation.

Acknowledgment. We acknowledge the support of the National Science Foundation, Grant CMMI 0826067, and the Department of Commerce via the National Textile Center, Grant No. M08-CL10. The authors would like to thank Bogdan Zdyrko, Ruslan Burtovyy, and Taras Andrukh for their assistance with the experimental setup.

Supporting Information Available: Different examples of surface instabilities observed at an interface between the electrolyte and fluid constituting products of electrochemical reaction on the anode surface during electropolishing of tungsten wires in 2 M KOH solution. This material is available free of charge via the Internet at http://pubs.acs.org.